DENTAL MATERIALS XXX (2006) XXX–XXX

available at www.sciencedirect.com

SCIENCE DIRECT®

journal homepage: www.intl.elsevierhealth.com/journals/dema

The effect of shot blasting and heat treatment on the fatigue behavior of titanium for dental implant applications

F. Javier Gil[a,*], *Josep A. Planell*[a], *Alejandro Padrós*[b], *Conrado Aparicio*[a]

[a] *Bioengineering Research Center (CREB), Department of Materials Science and Metallurgical Engineering, Universitat Politècnica de Catalunya, Avda. Diagonal 647, 08028-Barcelona, Spain*
[b] *Instituto Padrós, Barcelona, Spain*

ARTICLE INFO

Article history:
Received 8 April 2005
Received in revised form 2 December 2005
Accepted 8 March 2006

Keywords:
Titanium
Dental implants
Fatigue resistance
Shot blasting
Residual stresses

ABSTRACT

Objectives. The effect of shot blasting treatment on the cyclic deformation and fracture behavior of a commercial pure titanium with two different microstructures; equiaxed (α-phase) and acicular (martensitic α′-phase) was investigated.
Methods. Fatigue tests were carried out in artificial saliva at 37 °C. Cyclic deformation tests were carried out up to fracture and fatigue crack nucleation and propagation were analysed. Residual stresses were determined by means of X-ray diffraction.
Results. The results show that shot blasting treatment improves fatigue life in the different microstructures studied. The equiaxed phase has improved mechanical properties compared to the acicular one. Despite the fact that control of the variables of shot blasting is not precise because of the nature of the treatment, it improves the fatigue life by the fact that the initiation site of the fatigue crack changes from the surface of the specimen to the interior of the shot blasted specimen. This is a consequence of the layer of compressive residual stresses that the treatment generates on titanium surfaces. The acicular morphology of the martensite favors crack propagation along the interface of the α′ plates.
Significance. Shot blasting, which is widely used on titanium dental implants in order to favour their osseointegration, can also improve their fatigue resistance.

1. Introduction

The design of an oral implant device has always to take into consideration cyclic loading during the life in service of the implant, and therefore the fatigue endurance of the materials used will play a very important role when trying to estimate the long-term performance of the device. Thus the assessment of the fatigue behavior of implantable alloys has been taking on greater importance. Wrought cobalt–chromium, titanium and Ti–6Al–4V alloys show similar fatigue endurance, both when evaluated by means of rotary bending fatigue tests (about 550 MPa) [1], and when corrosion fatigue tested in torsion [2]. A relevant aspect is that the elastic modulus of titanium (110 GPa) is about half that of stainless steel (200 GPa) and also of cobalt–chromium–molybdenum alloys (235 GPa). This is a very important point to be taken into account when considering the load transfer into the bone when a dental implant, a joint prosthesis, or an osteosynthesis device is to be designed.

Table 1 summarizes the fatigue endurance for some of the alloys previously discussed. It should be pointed out that the fatigue strength limit is reduced in all cases when the material is tested in saline solution compared to tests performed in air. It should also be pointed out that both in air and in saline solution, titanium shows the highest fatigue strength limit compared to the rest of the exposed metals shown in Table 1.

* *Corresponding author.* Tel.: +34 93 4016708; fax: +34 93 4016706.
E-mail address: francesc.xavier.gil@upc.edu (F. Javier Gil).
0109-5641/$ – see front matter © 2006 Academy of Dental Materials. Published by Elsevier Ltd. All rights reserved.
doi:10.1016/j.dental.2006.03.003

Table 1 – Fatigue strength of some metals used for implants, in MPa

Material	In air	In saline solution
316L stainless steel (annealed)	260–280	230–270
Cast Co–Cr–Mo alloy	310	240–280
Wrought Co–Cr–Mo alloy	550	475
Wrought commercial pure Ti	300	240
Ti–6Al–4V	605	500

Moreover, titanium and titanium alloys can be strengthened and their mechanical properties varied by controlling their composition by means of thermomechanical processing techniques [3–8].

Titanium and titanium alloys are also resistant to general corrosion, pitting and crevice corrosion, which may occur in other alloys as a result of the aggressive attack of body fluids [9–11].

Because of all these properties, commercially pure titanium (c.p. Ti) is widely used as a dental implant material [12,13]. But clinical success is achieved not only because of the implant material but also due to other properties [14]. Among them, one of the most important is surface implant quality, which refers to its mechanical, physicochemical and topographic properties [15,16]. In this sense it is known that an increased implant-surface roughness enhances the in vitro behavior of osteoblasts [17–19]. Moreover, a better long-term in vivo response is achieved [20–24]. Osseointegration of the implant is meant to be achieved by bone in-growth into the roughness of the titanium surface [16,25].

Shot blasting is one of the most frequently used treatments for obtaining a rough surface of a dental implant [16,26]. The materials of the shot particles, which are bombarded onto the dental implant surface, are chemically stable materials that will not stimulate a negative response of the biological behavior of the implant [27]. Shot blasting induces a residual stress layer in the treated material because of the local plastic deformation of the metal [28]. Although the variables of shot blasting are not exhaustively controlled, as for shot peening [29], the stressed superficial layer is in compression and, consequently, an increase in the fatigue resistance of the shot blasted dental implant is expected.

The influence of the shot blasting treatment on the fatigue and fracture properties of titanium with different microstructures has been studied in this work.

2. Materials and methods

The c.p. Ti Grade III used in the present work was kindly donated by Klockner, S.A. The material came as cylindrical rods of 12 mm diameter, forged at 950 °C, subsequently annealed at 700 °C for 2 h and then cooled in air. The chemical composition of the alloy is shown in Table 2. The metallographic microstructure corresponds to equiaxed α-grains (Fig. 1). Both the composition and the microstructure satisfy the ASTM F67-00 [30] standard for unalloyed Ti for surgical implant applications.

Tensile specimens with a ratio diameter to gage length of 1/5 and fatigue specimens were machined. A first batch of specimens was kept as the as-received material, whilst second and third batches of specimens were heat treated. These specimens were kept for 1 h in a tubular furnace (HST16, Hobersal, Spain) in an argon atmosphere (99.9999%) at 1050 °C, which is a temperature just above the β-transus for the Ti, and they were then held in water at 20 °C. The resulting quenched microstructure corresponds to acicular α′-martensite (Fig. 2). The specimens of the third and fourth batches were shot blasted producing a roughened surface for the specimens in the two microstructures (equiaxed α-phase and acicular α′-martensite).

Table 2 – Chemical composition of the c.p. Ti used in this work

Element	wt.%
Nitrogen max.	0.05
Carbon max.	0.10
Hydrogen max	0.0125
Iron max.	0.30
Oxygen max.	0.35
Titanium max.	Balance

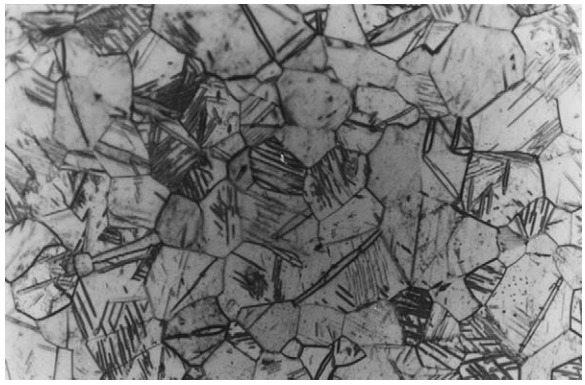

Fig. 1 – Microstructure of the equiaxed α-c.p. Ti.

The c.p. Ti Grade III discs were shot blasted with particles of Al_2O_3 and 600 μm in mean size, using 0.2 MPa of blast pressure.

Qualitative surface roughness was observed by scanning electron microscopy (SEM) (6400, Jeol, Japan), and quantitative surface roughness was determined by means of a profilometer with a diamond tip (Surftest SV500, Mitutoyo, Japan). R_a and other surface parameters were calculated. Energy dispersive

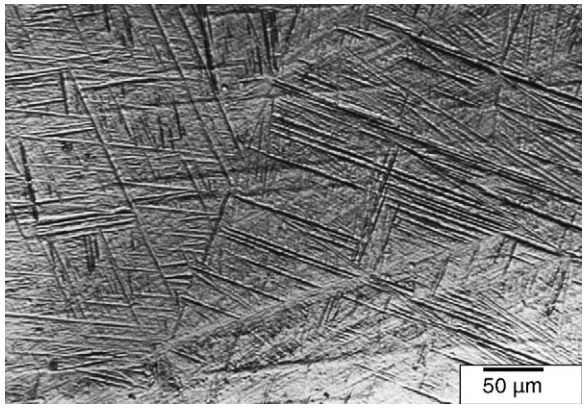

Fig. 2 – Microstructure of the acicular α′-martensite.

Table 3 – Chemical composition of the artificial saliva

Compound	Composition (g/dm^3)
K_2HPO_4	0.20
KCl	1.20
KSCN	0.33
Na_2HPO_4	0.26
NaCl	0.70
$NaHCO_3$	1.50
Urea	1.50
Lactic acid	Until pH 6.7

X-ray analysis was used for semi-quantitative surface chemical composition measurements (Analytical LZ5, Link, United Kingdom).

The hardness distribution in a cross-section of the shot blasted specimens was measured using a Vickers microhardness indentor (Akashi, Matsusawa, Japan) with a load of 100 gf. The time for indentation was 15 s.

Residual stresses were measured with a diffractometer incorporating a Bragg–Bentano configuration (D500, Siemens, Germany). The measurements were done for the family of planes (2 1 3), which diffracts at $2\theta = 139.5^\circ$. The elastic constants of Ti for this family of planes are $EC = (E/1+\nu)_{(2\,1\,3)} = 90.3$ (1.4) GPa. Eleven ψ angles, 0° and five positive- and five negative-angles were evaluated. The position of the peaks was adjusted with a pseudo-Voigt function using appropriate software (WinplotR, free access on-line), and then converted to interplanar distances (d_ψ) using Bragg's equation. The d_ψ versus $\sin^2\psi$ graphs and the calculation of the slope of the linear regression (A) were done with appropriate software (Origin, Microcal, USA). The residual stress is $\sigma = EC(1/d_0)A$; where d_0 is the interplanar distance for $\psi = 0^\circ$.

The tensile specimens were tested in a universal screw driven testing machine (Bionix, MTS, USA) of 100 kN capacity at a cross-head speed of 1 mm min^{-1}. The fatigue specimens were cyclically deformed in tension-compression under strain control $R_e = -1$, in a servo-hydraulic testing machine of 100 kN capacity using a container with artificial saliva at 37 °C. The chemical composition of the artificial saliva used is shown in Table 3. The strain rate was always kept constant at 6.5×10^{-3} s^{-1}. The total strain amplitude used was $\pm 7 \times 10^{-3}$. The deformed and fractured specimens were observed by means of SEM.

3. Results and discussion

The surface roughness of the as-machined metal for α-phase and α′-martensite are $R_a = 0.30$ (0.04) μm and $R_a = 0.33$ (0.03) μm, respectively. The shot blasted and α-phase specimens have $R_a = 4.2$ (0.8) μm, and the shot blasted and α′-martensite have $R_a = 3.8$ (0.7) μm. As expected, the shot blasted specimens have statistically significant ($p < 0.001$; Student's t-test) and higher surface roughness than the as-machined ones. Non-statistically significant differences in R_a-values between equiaxed and acicular phase c.p. Ti were found. The roughness obtained (chemical composition and size of shot particles and shot blasting pressure) for the shot blasted c.p. Ti was determined as optimal for in vitro and in vivo response in previous works [19,24].

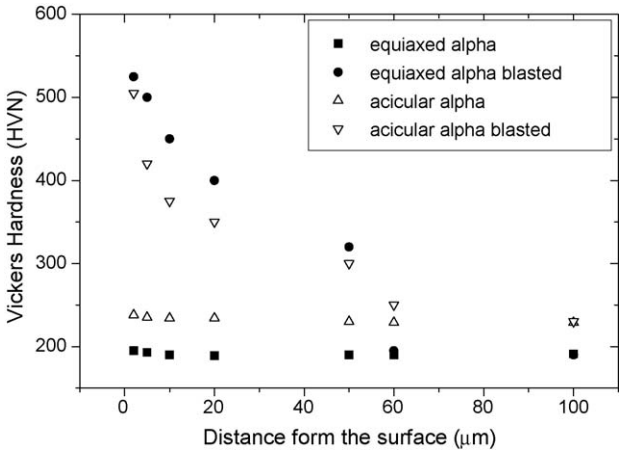

Fig. 3 – Hardness distribution at the above cross-section of a sample of the different the types of materials studied.

The hardness distribution at the above cross-section of the materials studied is presented in Fig. 3. The maximum hardness of 525 (13) HVN and 516 (26) HVN for equiaxed and acicular microstructures, respectively, with shot blasting treatment were measured near the surface. Hardness decreased gradually with increasing distance from the surface. The average hardness of the matrix for the equiaxed phase is 205 (9) HVN and for the acicular phase is 234 (11) HVN; so that the increase in hardness by shot blasting is, approximately, 300 HVN for the two microstructures.

Fig. 4 is an example of d_ψ versus $\sin^2\psi$ graph for a shot blasted α-phase c.p. Ti specimen showing the linear trend of the results with a negative slope. The linearity confirms the validity of the calculated value for the residual stresses and the negative slope indicates that the residual stresses are compressive. Fig. 5 shows an example of d_ψ versus $\sin^2\psi$ graph for an as-machined α-phase c.p. Ti specimen. In this case the results give a two-slope configuration, with a slope for the positive ψ angles and the other for the negative ψ angles. This two-slope configuration can be attributed to a surface with a high shear strain like the machined titanium. However, the

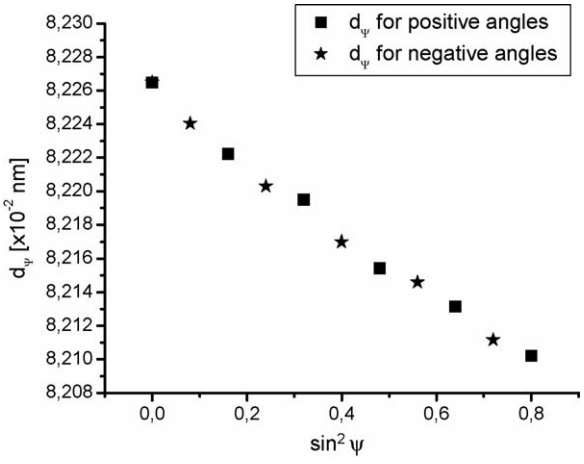

Fig. 4 – Example of d_ψ vs. $\sin^2\psi$ graph for a shot blasted α-phase c.p. Ti specimen.

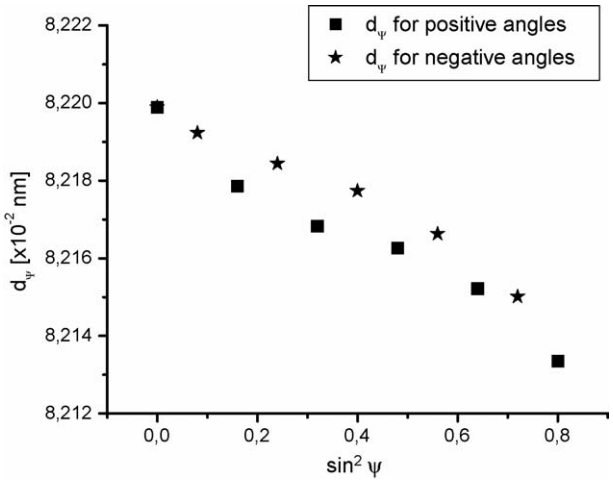

Fig. 5 – Example of d_ψ vs. $\sin^2 \psi$ graph for an as-machined α-phase c.p. Ti specimen.

Table 4 – Surface residual stresses calculated at the four different types of c.p. Ti studied

Material	σ (MPa)
α-Phase as-machined	−77.2 (5)
α′-Martensite as-machined	−69.3 (4)
α-Phase shot blasted	−220.0 (3)
α′-Martensite shot blasted	−205.1 (8)

slope of the curve is also negative indicating the compressive nature of the residual stresses induced by the machining. The values for the residual stresses are summarized in Table 4. As expected, the compressive stresses induced by shot blasting on c.p. Ti are statistically significant ($p < 0.001$; Student's *t*-test) and highly different from those induced on as-machined samples; but there are no statistically significant differences between equiaxed and acicular phase, both as-machined and shot blasted. All these results agree with the values obtained in hardness tests because the higher the hardness, the higher the compressive residual stresses. According to this, a compressive layer with a depth showed by the hardness profiles (Fig. 3) might be expected.

The different materials have been tested in unidirectional tension in order to obtain their monotonic stress–strain curves. The relevant parameters are listed in Table 5, where each value has been obtained from the average of two different tests for each material. A significant result is that acicular microstructures significantly reduce the ductility of the alloy.

Table 5 – Mechanical properties obtained from the tensile tests on the different materials studied

Material	Maximum strength (MPa)	Yield stress 0.2% (MPa)	Ductility (%)
α-Phase as-machined	460 (30)	155 (23)	46 (7)
α′-Martensite as-machined	570 (40)	175 (12)	26 (5)
α-Phase shot blasted	480 (39)	168 (25)	39 (4)
α′-Martensite shot blasted	587 (34)	189 (23)	19 (3)

Table 6 – Number of cycles to fatigue-failure (N_f) and cumulative plastic strain (ε_{cum}) for the different c.p. Ti studied

Material	N_f	ε_{cum}
Titanium alpha	35115 (1200)	3.7 (0.8)
Titanium acicular	24447 (1348)	2.6 (0.3)
Titanium alpha with blasting	51578 (2890)	2.9 (0.5)
Titanium acicular with blasting	37600 (1001)	1.9 (0.4)

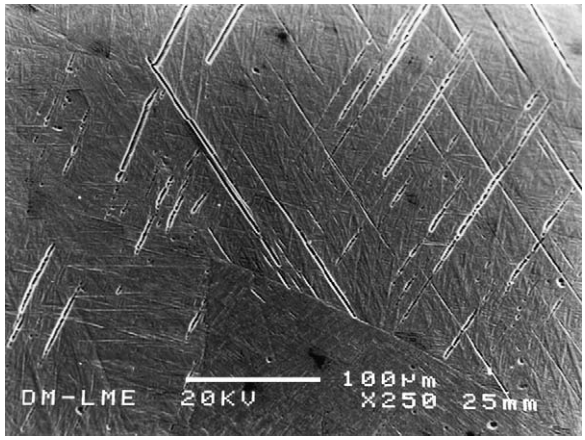

Fig. 6 – Crack propagation in the acicular c.p. Ti microstructure.

Table 6 shows the number of cycles to failure (N_f) and the cumulative plastic strain (ε_{cum}) for the α- and α′-microstructures without and with shot blasting treatment. It can be observed that the as-machined microstructure of the equiaxed phase presents longer fatigue life than the acicular microstructure. This is because the interface of the acicular phase is a fast way for the propagation of the fatigue crack, as can be observed in Fig. 6.

The fatigue behavior of the samples submitted to shot blasting treatment is better due to the compressive effect of the residual stresses on the surface, which makes crack nucleation difficult. This fact can be observed in Figs. 7 (as-machined specimen) and 8 (shot blasted specimen), where the crack grows from the surface and from 15 μm beneath the surface, respectively. As a consequence, an improvement

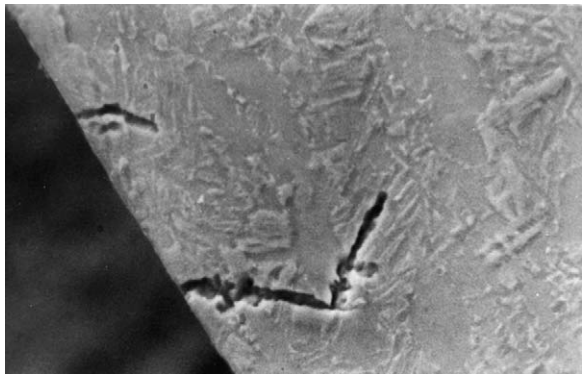

Fig. 7 – Crack nucleation on the surface of the specimen as-machined.

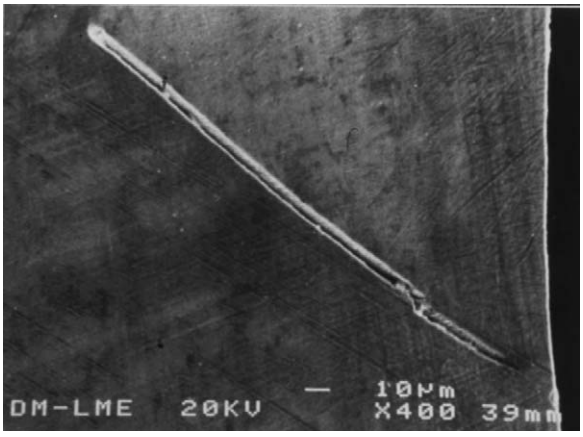

Fig. 8 – Crack nucleation beneath the surface of the shot blasted specimen.

in the fatigue behavior of the shot blasted treatment for the two microstructures studied (α-equiaxed and α′-acicular) is obtained. The crack propagation is very similar for the four specimens and can be observed in Fig. 9, where the crack propagation in the fracture surface with the grooves of each cycle can be seen.

The four types of specimens are cyclically deformed at different total strain amplitudes, and cyclic softening is observed in all cases. The maximum stress reached at every total strain amplitude is higher for the equiaxed than for the acicular microstructures. The highest rate of softening was observed for the acicular phase.

Consequently, shot blasting treatment increases the implant surface roughness by the impingement, at high pressure, of small abrasive particles, which results in local plastic strain. This fact will produce a firmer and earlier fixation and a better osseointegration of a dental implant as explained in the Introduction. Besides, this impingement produces an increase in the surface hardness due to the compressive load of the impact of the particles. Despite the fact that the variables of the shot blasting treatment are not exhaustively controlled, the value of the residual compressive stresses on the surface layer affected by the treatment suggests that the crack nucleation site changes from the specimen surface (for the as-machined metal) to the specimen interior (for the shot blasted metal). This change is postulated to result in a significant modification of fatigue properties of dental implants made of c.p. Ti.

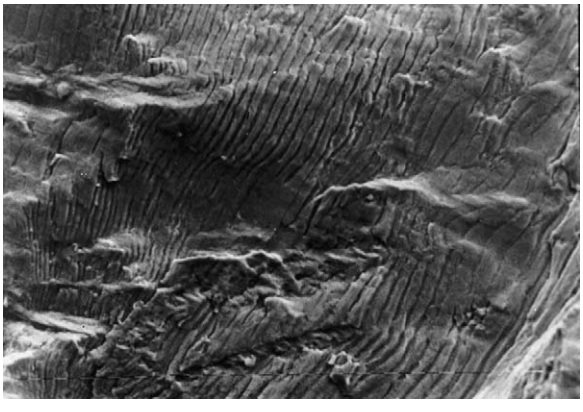

Fig. 9 – Fatigue crack propagation representative for all the materials studied.

4. Conclusion

Shot blasting of c.p. Ti dental implants not only improves the osseointegration of the implants because of the increase in the metal surface roughness but should also improve their fatigue life because of the layer of compressive residual stress that is formed.

Acknowledgements

The authors are grateful to the CICYT for funding the present work through project MAT2003-08165 and to Klockner, S.A. for kindly donating the material.

REFERENCES

[1] Manero JM, Gil FJ, Planell JA. Effect of saline solution environment on the cyclic deformation of Ti-6Al-4V. J Mater Sci: Mater Med 1996;7:131–4.
[2] Donachie MJ. In: Donachie MJ, editor. Titanium: a technical guide. Ohio: ASM; 1989.
[3] Blackburn MJ, Williams JC. Phase transformations in titanium alloys. Trans TMS-AIME 1967;239:1200–8.
[4] Collings EW. The physical metallurgy of titanium alloys. Ohio: ASM; 1984. pp. 321–354.
[5] Polmear IJ. Light alloys. In: Metallurgy of the light metals. Metallurgy and materials science series. London: Arnold; 1981. pp. 239–278.
[6] Gil FJ, Manero JM, Planell JA. Effect of heat treatment on the cyclic softening. In: Froes, Caplan, editors. Titanium 92. Science and technology. TMS; 1993. p. 1843–9.
[7] Semlitsch MF, Panic B, Weber H, Schoen R. Comparison of the fatigue strength of femoral prosthesis stems made of forged Ti–Al–V and cobalt base alloys. In: Luckey, Kubli, editors. Titanium alloys in surgical implants. ASTM-STP796. Philadelphia: ASTM; 1981. p. 120–35.
[8] Bannon BP, Mild EE. Titanium alloys for biomaterial application: an overview. In: Luckey, Kubli, editors. Titanium alloys in surgical implants. ASTM-STP796. Philadelphia: ASTM; 1981. p. 7–14.
[9] Pourbaix M. Electrochemical corrosion of metallic biomaterials. Biomaterials 1984;5:122–34.
[10] Tengvall P, Lundtröm I. Physico-chemical considerations of titanium as a biomaterial. Biomaterials 1992;9:115–34.
[11] Aparicio C, Gil FJ, Fonseca C, Barbosa M, Planell JA. Corrsoion behaviour of commercially pure tianium shot blasted with different materials and sizes of shot particles for dental implant applications. Biomaterials 2003;24:263–73.
[12] Brånemark PI, Hansson BO, Adell R, Breine U, Lindström J, Hallen O, Öhman A. Osseointegrated implants in the treatment of edentulous jaw. Experience from a 10-year period. Scand J Reconstr Surg 1977;(Suppl 16):1–132.
[13] Lemons JE. Application of materials in medicine and dentistry. Dental implants. In: Ratner BD, Hoffman AS, Schoen FJ, Lemons JE, editors. Biomaterials science: an introduction to materials in medicine. San Diego: Academic Press; 1996. p. 308–18.

[14] Albrektsson T, Brånemark PI, Hansson BO, Lindström J. Osseointegrated titanium implants. Acta Orthop Scand 1981;52:155–70.
[15] Thomas KA, Cook S. An evaluation of variables influencing implant fixation by direct bone apposition. J Biomed Mater Res 1985;19:875–901.
[16] Wennerberg A. On surface roughness and implant incorporation. PhD thesis. Göteborg, University of Göteborg; 1996.
[17] Anselme K. Osteoblast adhesion on biomaterials. Biomaterials 2000;21:667–81.
[18] Boyan BD, Lohmann CH, Dean DD, Sylvia VL, Cochran DL, Schwartz Z. Mechanisms involved in osteoblast response to implant surface morphology. Annu Rev Mater Res 2001;31:357–71.
[19] Aparicio C, Engel E, Gil FJ, Planell JA. Human-osteoblast proliferation and differentiation on grit-blasted and bioactive titanium for dental applications. J Mater Sci: Mater Med 2002;13:1105–11.
[20] Predecki P, Stephan JE, Auslander BA, Mooney VL, Kirkland K. Kinetics of bone growth into cylindrical channels in aluminium oxide and titanium. J Biomed Mater Res 1972;6:375–400.
[21] Wennerberg A, Albrektsson T, Johansson C, Andersson B. Experimental study of turned and grit-blasted screw-shaped implants with special emphasis on effects of blasting material and surface topography. Biomaterials 1996;17:15–22.
[22] Buser D. Titanium for dental applications (II). Implants with roughened surfaces. In: Brunette DM, Tengvall P, Textor M, Thomsen P, editors. Titanium in medicine: material science, surface science, engineering, biological responses and medical applications. Berlin: Springer Verlag; 2001. p. 875–88.
[23] Svehla M, Morberg P, Zicat B, Bruce W, Sonnabend D, Walsh WR. Morphometric and mechanical evaluation of titanium implant integration: comparison of five surface structures. J Biomed Mater Res 2000;51:15–22.
[24] Aparicio C, Gil FJ, Thams U, Muñoz F, Padrós A, Planell JA. Osseointegration of grit-blasted and bioactive titanium implants: histomorphometry in minipigs. Key Eng Mater 2004;254–256:737–40.
[25] Gotfredsen K, Nimb L, Hjorting-Hansen E, Jensen JS, Holmen A. Histomorphometric and removal torque analysis for TiO_2-blasted titanium implants. Clin Oral Implant Res 1994;5:202–6.
[26] Jones FH. Teeth and bones: applications of surface science to dental materials and related biomaterials. Surf Sci Rep 2001;42:75–205.
[27] Naji A, Harnad MF. Cytocompatibility of two coating materials, amorphous alumina and silicon carbide, using human differentiated cell cultures. Biomaterials 1991;12:690–4.
[28] Leliaert RM, Weightman N, Woelfel MM. Abrasive Blast Cleaning. In: ASM metals handbook, vol. 5, surface engineering. Metals Park: ASM International; 1995. pp. 83–96.
[29] Mehelich CS, Van Kuiken L, Woelfel MM. Shot peening. In: ASM metals handbook, vol. 5, Surface engineering. Metals Park: ASM International; 1995. pp. 138–149.
[30] ASTM F67-00, Standard specification for unalloyed titanium for surgical implant applications, 2000.